

Effects of the preparation method on the performance of the Cu/ZnO/Al₂O₃ catalyst for the manufacture of L-phenylalaninol with high ee selectivity from L-phenylalanine methyl ester

Cite this: *Catal. Sci. Technol.*, 2014, 4, 1132

Zhangping Shi,^a Xiuzhen Xiao,^{*a} Dongsen Mao^a and Guanzhong Lu^{*ab}

The effects of the preparation method on the properties of Cu/ZnO/Al₂O₃ catalysts for L-phenylalanine methyl ester hydrogenation to L-phenylalaninol were investigated in detail, including the precipitation method and conditions (the aging time, calcination temperature and so on), with the help of ICP-OES, N₂ and N₂O adsorption, XRD, H₂-TPR and TEM techniques. The results show that physicochemical properties of the catalysts are greatly affected by the preparation method and conditions. The uniform size distribution of CuO species can be obtained by fractional co-precipitation. The appropriate aging time is 2 h, and the catalyst aged for 2 h has the largest metallic copper surface area (S_{Cu}) and surface copper amount and the smallest CuO crystallites. The lower calcination temperature is favorable for increasing the surface area and metallic copper surface area of the catalyst. The spinel structure CuAl₂O₄ phase can form after calcination at 550 °C. The turnover frequency (TOF) values of L-phenylalaninol formed using different catalysts indicate the structurally sensitive character of the title reaction, and S_{Cu} is not the sole cause affecting the catalytic activities of the catalysts. B-TOF on the basis of the active sites (Cu⁰) in the boundary between CuO and ZnO or Al₂O₃ was proposed; the relationships of B-TOF with d_{CuO} (particle size of CuO) and S_{Cu} were established. Using the Cu/ZnO/Al₂O₃ catalyst prepared by fractional co-precipitation with aging at 70 °C for 2 h and calcination at 450 °C for 4 h, 83.6% selectivity to L-phenylalaninol without racemization was achieved.

Received 17th November 2013,
Accepted 21st January 2014

DOI: 10.1039/c3cy00937h

www.rsc.org/catalysis

1. Introduction

Chiral amino alcohols, especially L-phenylalaninol, are versatile intermediates and can be widely applied in pharmaceutical chemistry, fine chemistry and resolution of racemic mixtures, *etc.*^{1–3} They are also popularly used as efficient catalysts for asymmetric synthesis reactions.^{4–9} Therefore, the formation of chiral amino alcohols has become the subject of considerable interest. Generally, chiral amino alcohols can be prepared by the catalytic aminolysis of epoxides with excess amines at elevated temperatures^{10–14} and the reduction of the corresponding acids or esters.^{15–18} In the latter process, the metal hydrides are used as reducing agents, which are reactive at low temperatures thereby retaining the integrity of the stereogenic center. However, most of these metal hydrides are only utilized in the laboratory to produce chiral amino alcohols on a 100–150 g scale.

In recent years, increasing attention has been given to catalytic hydrogenation that is another attractive approach for obtaining chiral amino alcohols. Noble metal catalysts under relatively mild reaction conditions were used, such as Ru oxide^{19–21} or its complexes.^{3,22} However, the catalytic systems mentioned above are also not commercially available. Undoubtedly, it is necessary to design a highly efficient and stable catalyst for improving the catalytic hydrogenation of chiral amino esters in order to avoid these drawbacks.

It is well known that the copper-based catalysts exhibit an excellent catalytic performance for hydrogenation of esters under relatively harsh conditions,^{23–28} but hydrogenation of chiral esters has been barely reported. Brands *et al.*²⁹ reported that copper-containing catalysts can catalyze the selective hydrogenation of carbon–oxygen bonds and are relatively inactive for carbon–carbon bond hydrogenolysis. We have used Cu/ZnO/Al₂O₃ as the catalyst for hydrogenation of L-phenylalanine methyl ester to L-phenylalaninol, and a 69.2% yield of L-phenylalaninol with an ee value of 99.84% was achieved.³⁰ However, the selectivity to L-phenylalaninol is still lower. Previous research studies showed that the catalytic properties of Cu/ZnO/Al₂O₃ catalysts are affected by the

^a Research Institute of Applied Catalysis, School of Chemical and Environmental Engineering, Shanghai Institute of Technology, Shanghai 20023, PR China.
E-mail: gzhlu@ecust.edu.cn, jerryxiaozh@163.com; Fax: +86 21 60879111

^b Key Laboratory for Advanced Materials and Research Institute of Industrial Catalysis, East China University of Science and Technology, Shanghai 200237, PR China

preparation and reduction activation method of mixed oxides.³¹ For instance, Li and Inui³² found that the pH value of the reaction medium altered the phase composition of the catalyst, and the precipitation temperature affects the precipitation kinetics of the precursors of catalysts, while aging temperature determined phase inter-dispersion. Figueiredo *et al.*³³ reported that the inter-dispersion of oxide phases was influenced by the precipitation methods. Jung *et al.*³⁴ suggested that precursor structures would be changed during the aging process, and the metallic copper surface area was decreased due to a long aging time. Fujita *et al.*³⁵ investigated the effects of calcination and reduction conditions on the catalytic performance of the Cu/ZnO catalyst for the methanol synthesis from CO₂ and found that a highly efficient catalyst could be prepared from aurichalcite by controlling the preparation conditions. The reported results mentioned above show that the catalytic properties of Cu/ZnO/Al₂O₃ are affected remarkably by the preparation method and conditions.

Herein, the Cu/ZnO/Al₂O₃ catalysts were prepared using different precipitation methods and conditions, their physicochemical and catalytic properties for hydrogenation of L-phenylalanine methyl ester to L-phenylalaninol were investigated, and the overall reactions are given in Scheme 1. The effects of the physicochemical properties of catalysts on their catalytic performances were discussed.

2. Experimental section

2.1. Catalyst preparation

The Cu/ZnO/Al₂O₃ catalysts with optimal mole ratio of Cu : Zn : Al = 1 : 0.3 : 1 were prepared with Cu(NO₃)₂·3H₂O, Zn(NO₃)₂·6H₂O, Al(NO₃)₃·9H₂O and Na₂CO₃ (A.R., Sinopharm Chemical Reagent Ltd.),³⁰ and the preparation procedures were as follows:

1.0 M Cu(NO₃)₂, 1.0 M Zn(NO₃)₂, 1.0 M Al(NO₃)₃ and 0.5 M Na₂CO₃ aqueous solutions were prepared first. Four different preparation methods were used as follows:

(a) 0.5 M Na⁺ aqueous solution was added to a mixture solution containing Cu²⁺, Zn²⁺ and Al³⁺ under stirring at 70 °C until the pH value of the reaction medium reached 7.5.

(b) The mixture solution of Cu²⁺, Zn²⁺ and Al³⁺ was added to the 0.5 M Na⁺ solution under stirring at 70 °C until the pH value of the reaction medium reached 7.5.

(c) The mixture solution of Cu²⁺, Zn²⁺ and Al³⁺ and the 0.5 M Na⁺ solution were added to the precipitating reactor under stirring at 70 °C, while the pH value of the reaction medium was kept at 7.5 from beginning to end.

(d) The mixture solution of Cu²⁺ and Zn²⁺ and the 0.5 M Na⁺ solution were co-precipitated at 70 °C and pH 7.5 under stirring. And the Al³⁺ solution and 0.5 M Na⁺ solution were co-precipitated under the same precipitation conditions described above. Then two solutions obtained above were mixed under the same conditions.

Then, these reaction media were aged under stirring for 5 h at 70 °C and cooled statically for 1 h. After filtration and washing with de-ionized water until the filtrate was neutral, the precursor was dried at room temperature for 12 h, then dried at 120 °C for 24 h, heated to 450 °C at 5 °C min⁻¹ and calcined at 450 °C for 4 h. The calcined catalyst was pressed and crushed to small-sized particles of 0.45–0.85 mm (20–40 mesh).

The prepared catalysts were labeled as CZA-x-y-t: x represents the precipitation method (a, b, c and d), y represents the aging time (5 h) at 70 °C, and t represents the calcination temperature (450 °C) for 4 h. Hence, four catalysts above are CZA-(a, b, c, d)-5-450.

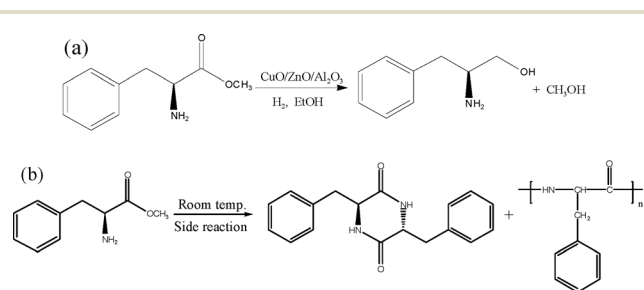
For the CZA-d-y-450 catalyst, the aging time (y) was changed from 0 to 5 h. The CZA-d-2-t catalyst aged for 2 h at 70 °C was calcined at 350–750 °C for 4 h.

2.2. Catalyst characterization

The chemical composition of the sample was determined by inductively coupled plasma-optical emission spectroscopy (ICP-OES; Perkin Elmer, Optima 7000 DV). The powder X-ray diffraction (XRD) patterns of the catalysts were recorded using a PANalytical X'Pert Pro MRD X-ray diffractometer (The Netherlands) with CuK α radiation ($\lambda = 0.154056$ nm) operated at 40 kV and 40 mA. The average crystalline sizes of catalysts (d_{CuO}) were calculated by the Scherrer equation based on the diffraction peak broadening. The surface areas of the catalysts were measured by N₂ adsorption at -196 °C using a Micrometrics ASAP 2020 apparatus and calculated by the Brunauer–Emmett–Teller (BET) method.

The metallic copper surface area (S_{Cu}) of the catalyst was determined using a nitrous oxide chemisorption method called the reactive frontal chromatography (RFC) technique.³³ For example, 200 mg of sample was reduced in a 5% H₂/He stream at a heating rate of 5 °C min⁻¹ to 300 °C and maintained for 1 h. After that, the reactor was purged with the pure He stream and cooled down to 60 °C, and then N₂O titration was carried out. The surface copper atoms density of 1.46×10^{19} copper atoms per m² assuming Cu:N₂O = 2:1 was used for the calculation of the copper surface area. The copper dispersion (D_{Cu}) was defined as the amount of the exposed copper in relation to the total amount of copper atoms of the catalyst.

Transmission electron microscopy (TEM) images were obtained using a JEOL 1400 microscope operated at 100 kV. The samples were suspended in ethanol and supported onto a holey carbon film on a Cu grid.



Scheme 1 (a) Hydrogenation of L-phenylalanine methyl ester to L-phenylalaninol and (b) the side reaction of L-phenylalanine methyl ester self-polymerization.³⁶

H₂-temperature-programmed reduction (H₂-TPR) was performed using a continuous-flow apparatus equipped with a thermal conductivity detector (TCD). 30 mg of catalyst was used and pretreated at 350 °C for 1 h under a N₂ flow of 30 mL min⁻¹. After it was cooled to 50 °C under N₂, it was flushed by a 10% H₂/N₂ flow of 30 mL min⁻¹ instead of pure N₂, and TPR of the sample was run from 50 to 550 °C at 5 °C min⁻¹.

2.3. Catalytic activity testing

The activity of the catalyst for L-phenylalanine methyl ester hydrogenation was tested in a 500 mL stainless steel autoclave under stirring at a speed of 500 rpm. After 1.0 g of catalyst (20–40 mesh) was packed in the reactor, this reactor was flushed with 4 MPa H₂ to expel air 4 times and the catalyst was reduced in 1 MPa H₂ at 250 °C for 4 h, and then the reactor was cooled to room temperature. 1.5 g of L-phenylalanine methyl ester (liberated from the L-phenylalanine methyl ester hydrochloride with 0.5 M Na₂CO₃ aqueous solution and extracted by ethyl acetate) diluted in 150 mL ethanol was introduced, that is, L-p/Cat. = 1.5 (mass ratio). The typical reaction conditions were 4 MPa of H₂ and 110 °C. After the reaction was over, the reactor was cooled to room temperature, and then the pressure was released. The catalyst was separated by centrifugation, and the products were analyzed by HPLC and NMR (Bruker, AVANCE III 500 MHz).

HPLC (high performance liquid chromatography) analysis was done using an Agilent 1260 Infinity equipped with an ultraviolet detector and a column (Poroshell 120 EC-C18, 50 × 4.6 mm, 2.7 μm particle size). The operating conditions of HPLC were as follows: the mobile phase was 0.05 mol L⁻¹ ammonium acetate aqueous solution (pH = 5.0) containing 5 vol.% methanol, the flow rate was 0.6 mL min⁻¹, the detection wavelength was 254 nm and the column temperature was 35 °C. Experimental errors for the conversion and selectivity are within ±2%. The conversion of L-phenylalanine methyl ester (L-p) (*C*), yield of L-phenylalaninol (L-p-ol) (*Y*) and chemoselectivity (*S*) were calculated as follows:

$$C (\%) = (\text{the mass of L-phenylalanine methyl ester converted} / \text{total mass of L-phenylalanine methyl ester in the feed}) \times 100\%$$

$$Y (\%) = (\text{the mass of L-phenylalaninol formed actually} / \text{the mass of L-phenylalaninol formed theoretically}) \times 100\%$$

$$S (\%) = (Y/X) \times 100\%$$

The ee value of the product was determined by HPLC with a chiral column (CHIRALPAK ID-3, 150 × 4.6 mm, 5 μm particle size) under the operating conditions: the mobile phase was the mixture solution (water/methanol = 70:30 (v/v), 0.6 mL min⁻¹) containing 3% triethylamine, the detection wavelength was 258 nm and the column temperature was 40 °C.

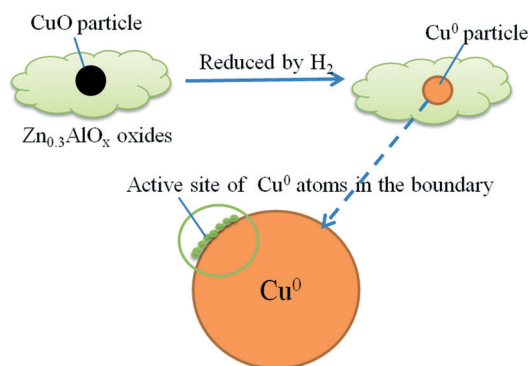
2.4. The structure and ee value of the product

The ¹H NMR spectrum of product L-phenylalaninol was obtained using a Bruker AVANCE-III 500. ¹H NMR (CDCl₃): 7.21–7.35 (5H, m, Ph-H), 3.42–3.68 (2H, m, -CH₂-O-), 3.15 (1H, s, -CH-N-), 2.53–2.84 (2H, m, CH₂-Ph), 1.83 (2H, b, -NH₂). In the product solution, only L-phenylalaninol could be detected

by HPLC with a chiral column, which indicates that the ee value is ~100% and chirality of the reactant can be well maintained after the reaction.

2.5. Boundary-turnover frequency (B-TOF)

Herein, we propose the boundary-turnover frequency (B-TOF) of L-phenylalaninol formation, which means the number of L-phenylalaninol molecules formed per second per metallic copper atom in the boundary between CuO and ZnO or Al₂O₃. Being different from TOF, B-TOF is calculated on the Cu sites in the boundary rather than on all Cu sites on the whole surface. The Cu sites in the boundary can be described ideally as the following figure:



In this model, CuO particles (or Cu⁰ particles) are located on the surface of Zn_{0.3}AlO_x oxide. The Cu⁰ particles are hypothesized as round particles, and their particle diameter was determined by the XRD patterns and the Scherrer equation. The active sites are Cu⁰ atoms in the boundary between CuO and the support, namely, the Cu⁰ atoms on the circumference of the round Cu⁰ particles on Zn_{0.3}Al₁O_x. The Cu⁰ atoms in the boundary between CuO and Zn_{0.3}Al₁O_x were calculated by:

$$N = S_{\text{CuO}} / \pi(d/2)^2 \times (\pi d/2r) = 2 \times S_{\text{CuO}} / (d \times r)$$

S_{CuO} = the surface area of CuO on the surface;

d = CuO average particle diameter determined by XRD data;

r = the radius of the CuO molecule, which is approximately equal to the O²⁻ ion radius (0.138 nm).

$$S_{\text{CuO}} = (S_{\text{Cu}}/a_1) \times a_2 = S_{\text{Cu}} \times a_2/a_1$$

S_{Cu} = the surface area of copper on the surface;

a_1 = the surface area of the copper atom (7.11×10^{-20} m²);

a_2 = the surface area of the CuO molecule, which is approximately equal to the surface area of the O²⁻ ion (5.98×10^{-20} m²).

3. Results and discussion

3.1. Effect of precipitation methods

To ascertain an appropriate reaction time, the effect of the reaction time on the title reaction over the CZA-d-5-450 catalyst was tested and the results are shown in Fig. 1A. The results show that the selectivity to L-phenylalaninol (L-p-ol) is hardly changed (~67.9%) and the conversion of L-phenylalanine methyl ester (L-p) is increased gradually with increasing reaction time. It reaches 96.3% after 4 h of reaction and ~100%

for 5 h. The results demonstrate that the *L*-phenylalaninol formed undergoes no further reaction at the applied conditions, that is to say, the surface Cu⁰ atoms are inactive for deep hydrogenation of *L*-phenylalaninol. Hence, the selectivity to *L*-phenylalaninol is not changed with the reaction time.

The catalytic performances of the CuZn_{0.3}AlO_x (CZA) catalysts prepared by different precipitation methods for *L*-phenylalanine methyl ester hydrogenation to *L*-phenylalaninol are presented in Fig. 1B. It can be seen that 100% conversion of *L*-phenylalanine methyl ester (*L*-p) was obtained at 110 °C and 4 MPa of H₂ for 5 h, and when the reaction time was decreased to 10 min, only 21.3–25.0% conversion was obtained. However, the reaction time hardly affected the selectivity to *L*-phenylalaninol (*L*-p-ol), which is only 50.6–67.9%.

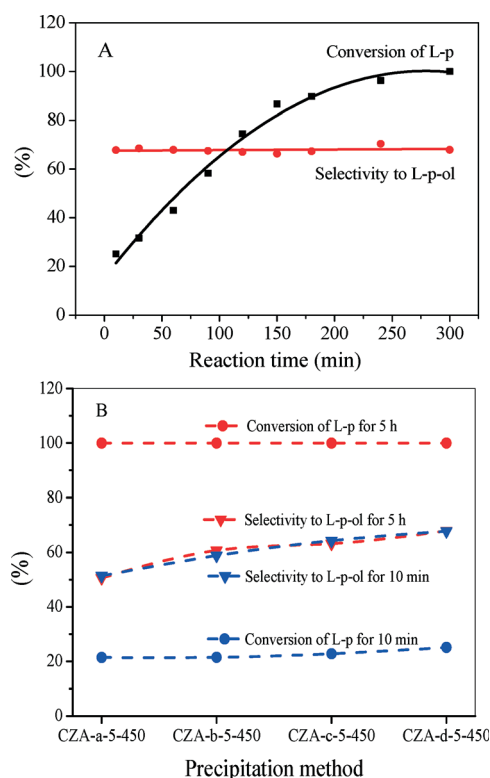


Fig. 1 The effect of reaction time on the *L*-phenylalanine methyl ester hydrogenation over the CZA-d-5-450 catalyst (A); effect of the precipitation method on the performance of the CZA catalyst (B) at 110 °C and 4 MPa of H₂ for 10 min or 5 h (*L*-p/Cat. = 1.5, wt.).

The results in Fig. 1B show that the precipitation method affects obviously the performance of the CZA catalyst, and among the four catalysts, the CZA-d-5-450 catalyst exhibits the highest activity, for instance, after reaction for 10 min, 67.9% selectivity and 25% conversion can be obtained.

The effect of the precipitation method on some physicochemical properties of the CZA catalysts is shown in Table 1. The elemental analysis results indicate that the precipitation method hardly affects the compositions of those catalysts. However, the BET surface area, average size of CuO crystallites (d_{CuO}), metallic copper surface area (S_{Cu}) and copper dispersion (D_{Cu}) of the CZA catalyst are obviously affected by the precipitation method. The BET surface areas are varied in the order of CZA-d-5-450 (159 m² g⁻¹) > CZA-c-5-450 (115) > CZA-b-5-450 (82.2) > CZA-a-5-450 (47.6), resulting in the similar variation of S_{Cu} and D_{Cu} values of these catalysts. For instance, for d_{CuO} estimated by the Scherrer equation on the basis of the XRD diffraction peak of CuO, CZA-a-5-450 is 22.3 nm and CZA-d-5-450 is only 10.5 nm. The results above show that the CZA sample (as CZA-d-5-450) prepared by mixing the co-precipitate of Cu and Zn with the Al-precipitate possesses larger dispersion and surface area of metallic copper, which are similar to the results reported by Figueiredo.³³

Different precipitation methods mean that the Cu, Zn and Al ions are deposited at different pH environments. Based on the different solubility product constants (K_{sp}) of Cu(OH)₂, Zn(OH)₂ and Al(OH)₃, the beginning precipitation pH of Cu²⁺ (as well as Al³⁺) is near 4 and that of Zn²⁺ is 6. During the precipitation of CZA-a-5-450, pH of the reaction medium was increased from 2.5 to 7.5, which would produce an inhomogeneous precipitation of Cu²⁺ with Zn²⁺ ions, resulting in weaker interaction of CuO and ZnO species. Hence, larger sizes and lower dispersion of CuO species were obtained for the CZA-a-5-450 sample.

During the precipitation of CZA-b-5-450, pH of the reaction medium was decreased from 11.5 to 7.5 and homogeneous distribution of the CuO species was obtained, but the size of the CuO phase is larger than that in CZA-c-5-450 (deposited at unvaried pH 7.5) and CZA-d-5-450, because each component can be completely precipitated under the higher pH value solution. In the preparation process of CZA-d-5-450, the co-precipitate of Cu/Zn and the Al-precipitate were formed separately, and then two precipitates were mixed uniformly,

Table 1 Physicochemical properties of the Cu/ZnO/Al₂O₃ catalysts prepared by different precipitation methods

Catalyst	Molar composition ^a			S_{BET} (m ² g ⁻¹)	d_{CuO} (nm)	S_{Cu} (m ² g ⁻¹)	D_{Cu} ^b (%)	TOF × 10 ^{3c} (s ⁻¹)	B-TOF ^d (s ⁻¹)
	Cu	Zn	Al						
CZA-a-5-450	1.03	0.30	0.97	47.6	22.3	4.6	2.2	13.5	0.492
CZA-b-5-450	1.06	0.30	0.94	82.2	13.9	6.3	3.0	11.2	0.254
CZA-c-5-450	1.05	0.28	0.97	115	11.6	8.1	3.9	10.3	0.197
CZA-d-5-450	1.00	0.28	1.02	159	10.5	11.5	5.5	8.4	0.140

^a Determined by the ICP-OES method. ^b D_{Cu} = exposed Cu atoms/total Cu atoms. ^c Turnover frequency (TOF) represents the number of *L*-phenylalaninol molecules formed (reaction for 10 min) per second per surface metallic copper atom. ^d B-TOF represents the number of *L*-phenylalaninol molecules formed (reaction for 10 min) per second per Cu⁰ atom in the boundary between CuO and ZnO or Al₂O₃.

which is not only beneficial for the dispersion between Cu–Zn–O and Al oxide species but also enhances the interaction of CuO with ZnO, resulting in the higher dispersion and smaller size of CuO crystallites in the CZA-d-5-450 sample. Therefore, it is easily understood that the CZA-d-5-450 sample exhibits higher catalytic activity and selectivity to the product, because a higher dispersion of Cu usually results in a higher catalytic performance for Cu-based catalysts.^{37–39}

Fig. 2 shows the XRD patterns of the catalysts prepared by different precipitation methods. The results show that no diffraction peaks of Al₂O₃ and ZnO can be detected, suggesting that Al₂O₃ and ZnO phases are amorphous or highly dispersed. The diffraction peaks of CuO can be observed at $2\theta = 35.6^\circ$, 38.8° (JCPDS 80-1268) in these catalysts. From CZA-a-5-450 to CZA-d-5-450, the diffraction peaks of CuO become weaker and broader, indicating a decrease in the CuO crystal size (Table 1).

Fig. 3 shows the TEM images of the Cu/ZnO/Al₂O₃ catalysts prepared by different precipitation methods. It can be seen that the precipitation methods have a great influence on the particle size and the distribution of catalysts. Among the four samples, the CZA-b-5-450 particle size seems generally relatively larger because of the higher pH value of the reaction medium, and the CZA-c-5-450 and CZA-d-5-450 samples exhibit smaller sizes. However, CZA-c-5-450 exhibits uniform size distribution with some bigger particles. For the CZA-d-5-450

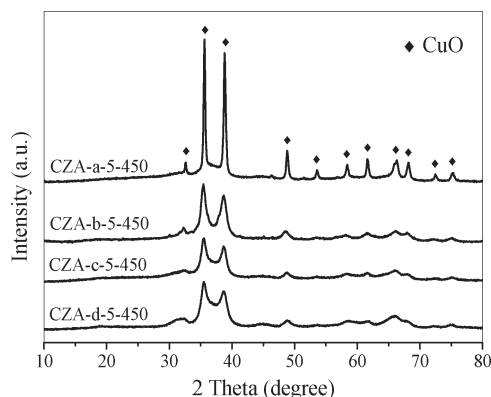


Fig. 2 XRD patterns of the Cu/ZnO/Al₂O₃ catalysts prepared by different precipitation methods.

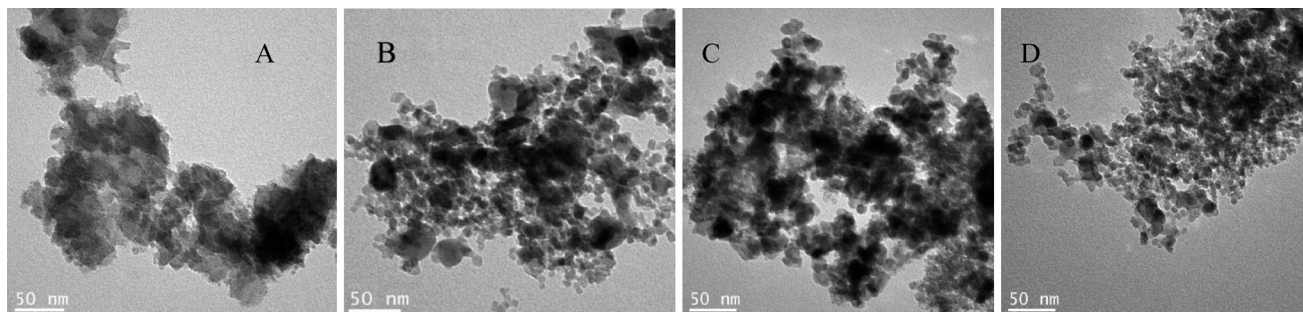


Fig. 3 TEM images of (A) CZA-a-5-450, (B) CZA-b-5-450, (C) CZA-c-5-450 and (D) CZA-d-5-450.

sample, the homogeneous and smallest particle size can be observed.

The H₂-TPR profiles of calcined catalysts are shown in Fig. 4, and four samples exhibit four different kinds of H₂ reduction (consumption) peaks at 150–275 °C, which can be deconvoluted to two (α and β) peaks and their peak positions and contributions are summarized in Table 2. Since ZnO and Al₂O₃ cannot be reduced in this temperature region,⁴⁰ these reduction peaks are only ascribed to the reduction of CuO species. The low temperature peak (α peak) is ascribed to the reduction of highly dispersed CuO, and the peak at higher temperature (β peak) is due to the reduction of bulk CuO.^{38,41} Compared with the reduction (reduction temperature is usually at ~300 °C) of pure CuO,⁴² CuO species in the CZA catalysts can be reduced at much lower temperatures, which suggests

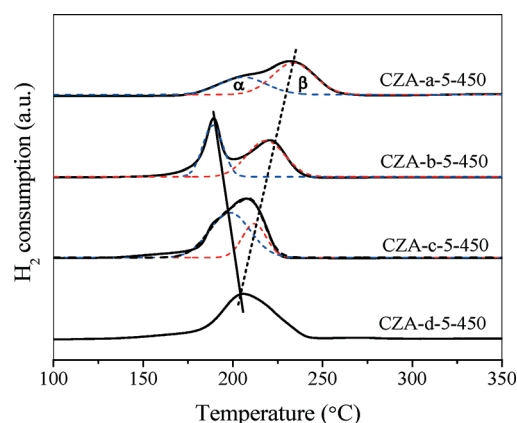


Fig. 4 H₂-TPR profiles of Cu/ZnO/Al₂O₃ catalysts prepared by different precipitation methods.

Table 2 Top temperatures and relative peak areas in the TPR patterns of Cu/ZnO/Al₂O₃ catalysts

Catalyst	T_α (°C)	T_β (°C)	$A_\alpha/(A_\alpha + A_\beta)^a$ (%)
CZA-a-5-450	206	234	35.5
CZA-b-5-450	191	218	43.5
CZA-c-5-450	189	212	69.4
CZA-d-5-450	206	—	—

^a A is the reduction peak area.

that the presence of ZnO can enhance the reducibility of CuO species.^{41,43–46}

The results in Fig. 4 show that the precipitation method affects remarkably the reduction properties of CZA catalysts. For CZA-a-5-450, CZA-b-5-450 and CZA-c-5-450 catalysts, there are obviously two reduction peaks, and in the TPR curve of the CZA-d-5-450 catalyst, two reduction peaks (α , β) have overlapped, which indicate that the former three samples contain two kinds of CuO species and the latter exists as almost one kind of CuO species. Although the top temperature of the β peak is related to the X-ray diffraction peak intensity of CuO (Fig. 2), we find that the higher the β peak temperature is, the stronger the diffraction peak of CuO is. That is to say, the β peak is attributed to the reduction of bulk CuO. Likewise, the larger the α peak area is, the larger the surface area of Cu (S_{Cu} , Table 1) is. In the TPR curve of the CZA-d-5-450 catalyst, only one peak is observed and the α peak is completely overlapping with the β peak, suggesting the presence of uniform particles of CuO species. Therefore CZA-d-5-450 possesses the largest S_{Cu} and the smallest crystallite size of CuO among the four samples.

Relating the catalytic activity data in Fig. 1 with S_{Cu} values in Table 1, it can be seen that the selectivity to L-phenylalaninol increases with the increase in the S_{Cu} values, but there is no linear relationship between selectivity and S_{Cu} . This indicates that the activity of the Cu/ZnO/Al₂O₃ catalyst is not only related to S_{Cu} but also to other factors, such as the promotional role of ZnO on the Cu sites, which can enhance the reducibility of the copper oxide phase with the help of the synergetic effect or the interaction between metallic copper and zinc oxide.^{30,40} It is well known that the interaction between the components of a catalyst can be selectively affected by different precipitation methods.³³ For the CZA-d-5-450 catalyst prepared by mixing the co-precipitate of Cu and Zn with the Al-precipitate, the interaction of CuO (or Cu) with ZnO ought to be stronger than other catalysts, which brings well into play the promotional role of ZnO.

3.2. Effect of precipitate aging time

The CZA-d-y-450 sample was used as the model catalyst, and the effect of the aging time on its catalytic performance is

shown in Fig. 5. It can be seen that 100% conversion of L-phenylalanine methyl ester can be obtained at 110 °C and 4 MPa of H₂ for 5 h, and over the CZA-d-2-450 aged for 2 h the selectivity to L-phenylalaninol reaches the highest (83.1%). When the reaction time was shortened to 10 min, the product selectivity curve is similar to that of 5 h. However, the conversions are decreased to 22–25% due to shorter reaction time. With the increase in the aging time from 0 h to 2 h, the conversion is increased from 22.1 to 25.4%, and with a further increase in the aging time, the conversion is no longer obviously changed. Therefore, the appropriate aging time is 2 h for the CZA-d-y-450 catalyst.

The main physicochemical properties of the CZA-d-y-450 catalysts with different aging times are shown in Table 3. The results show that the aging time hardly affects the Cu, Zn and Al contents in the catalyst, but its BET surface area is influenced remarkably and increased from 41.2 to 159 m² g⁻¹ with the increase in aging time from 0 to 5 h. The average crystallite size (d_{CuO}) of CuO declines from 23.0 to 10.2 nm with an increase in the aging time from 0 to 2 h, and with a further increase in the aging time, d_{CuO} is no longer significantly changed. The metallic copper surface area (S_{Cu}) of CZA-d-2-450 aged for 2 h reaches its maximum (16.6 m² g⁻¹), and the corresponding D_{Cu} (exposed copper atoms/total copper atoms) is also at its maximum (7.9%). In addition, we still

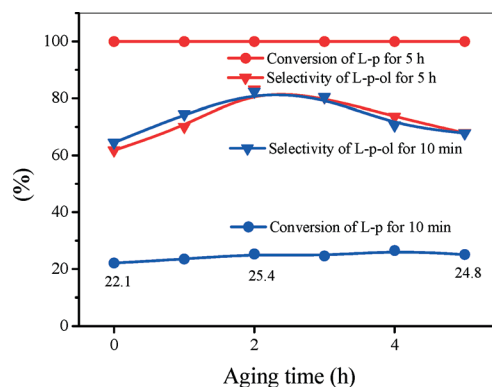


Fig. 5 Effect of the aging time at 70 °C on the performance of the CZA-d-y-450 catalyst for the hydrogenation of L-phenylalanine methyl ester at 110 °C and 4 MPa of H₂ for 10 min and 5 h (L-p/Cat. = 1.5, wt.).

Table 3 Physicochemical properties of the CZA-d-y-450 catalysts prepared with different aging times

Catalyst	Aging time (h)	Molar composition ^a			S_{BET} (m ² g ⁻¹)	d_{CuO} (nm)	S_{Cu} (m ² g ⁻¹)	D_{Cu} ^b (%)	TOF × 10 ^{3c} (s ⁻¹)	B-TOF ^d (s ⁻¹)
		Cu	Zn	Al						
CZA-d-0-450	0	0.97	0.31	1.02	41.2	23.0	7.4	3.5	10.9	0.402
CZA-d-1-450	1	1.02	0.30	1.07	53.4	12.6	12.4	5.9	8.0	0.160
CZA-d-2-450	2	1.03	0.29	0.98	92.0	10.2	16.6	7.9	7.0	0.114
CZA-d-3-450	3	1.02	0.29	1.01	99.7	10.7	14.9	7.1	7.5	0.140
CZA-d-4-450	4	1.07	0.30	1.01	126	10.4	13.5	6.5	7.8	0.121
CZA-d-5-450	5	1.04	0.28	1.02	159	10.5	11.5	5.5	8.4	0.140

^a Determined by the ICP-OES method. ^b D_{Cu} = exposed Cu atoms/total Cu atoms. ^c Turnover frequency (TOF) represents the number of L-phenylalaninol molecules formed (reaction for 10 min) per second per surface metallic copper atom. ^d B-TOF represents the number of L-phenylalaninol molecules formed (reaction for 10 min) per second per Cu⁰ atom in the boundary between CuO and ZnO or Al₂O₃.

found that the color of the precursor varied with the aging time, which means that the structure of the precursors changes during the aging process.^{34,47} Relating the catalytic activity data in Fig. 5 with S_{Cu} values in Table 3, it can be seen that the selectivity to *L*-phenylalaninol increases with an increase in S_{Cu} , and the CZA-d-2-450 catalyst with the largest S_{Cu} shows the highest catalytic performance.

The XRD patterns in Fig. 6 show that no diffraction peaks of Al_2O_3 , ZnO and $\text{Cu}_2\text{Al}_2\text{O}_4$ phases can be observed in the CZA-d- y -450 samples, like the XRD curve of the CZA-d-5-450 catalyst (Fig. 2). And the diffraction peaks of the CuO phase markedly decreased with an increase in the aging time from 0 to 2 h, due to a change of d_{CuO} . With a further increase in the aging time (> 2 h), the d_{CuO} values slightly increase with the aging time, but its variation is unapparent. Furthermore, the TEM images in Fig. 7 show that the particle size of CZA-d-2-450 is smaller than that of CZA-d-5-450, suggesting that increasing aging time (> 2 h) slightly contributes to the growth of catalyst particles.

Fig. 8 shows the H_2 -TPR profiles of the catalysts prepared with different aging times. All of the samples exhibit a broad reduction peak at 150–275 °C. The CZA-d-0-450 sample exhibits the highest reduction temperature, and the top reduction temperature of the CZA-d-2-450 sample aged for 2 h is the lowest. For other samples aged for >2 h, the top temperature of reduction peak rises with an increase in the aging time, although their XRD patterns are hardly changed (Fig. 6). Kniep *et al.*⁴⁸ reported that continuous precipitation aging would lead to a decreasing amount of Zn in the copper clusters for the Cu/ZnO catalysts. This shows that a long aging time is not beneficial for reducibility of copper oxide, because decreasing the Zn amount in CuO crystallites weakens the synergetic effect and hydrogen spillover between metallic copper and zinc oxide.

3.3. Effect of calcination temperature

On the basis of the results above, the CZA-d-2-450 prepared with aging time of 2 h was used a model catalyst to study the effect of the calcination temperature on its catalytic

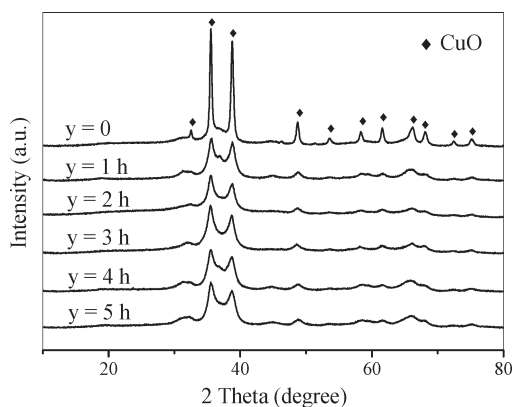


Fig. 6 XRD patterns of the CZA-d- y -450 catalysts prepared with different aging times (y).

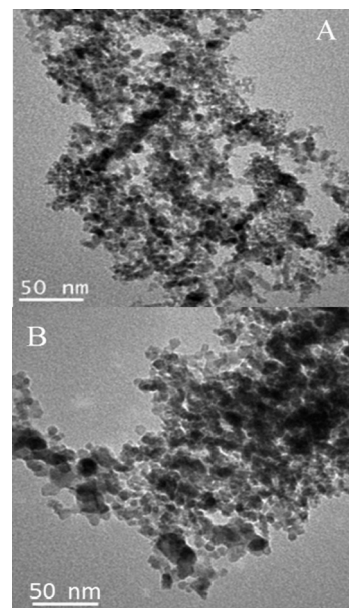


Fig. 7 TEM images of (A) CZA-d-2-450 and (B) CZA-d-5-450.

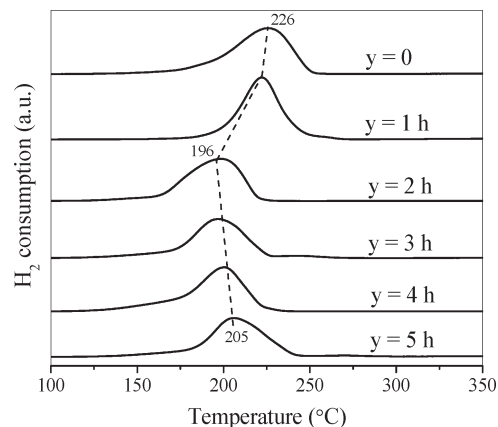


Fig. 8 H_2 -TPR patterns of the CZA-d- y -450 catalysts prepared with different aging times (y).

performance, and the results are shown in Fig. 9. The results show that 100% conversion of *L*-phenylalanine methyl ester can be obtained for all catalysts after 5 h of reaction, and the highest selectivity to *L*-phenylalaninol can be obtained over the CZA-d-2-450 catalyst calcined at 450 °C. If the calcination temperature was >450 °C, the catalytic activity of CZA-d-2- t would drastically decrease with an increase in calcination temperature. When the reaction time was shortened to 10 min, the product selectivity curve is similar to that after 5 h of reaction, and the conversions are decreased to 17–25.3%. Among those catalysts, the CZA-d-2-450 catalyst calcined at 450 °C exhibits the highest reactant conversion and product selectivity. Therefore, the appropriate calcination temperature is 450 °C.

For the CZA-d-2-450 catalyst, the effect of the reaction time on the conversion and product selectivity is given in Fig. 10. The results show that the selectivity to *L*-phenylalaninol is

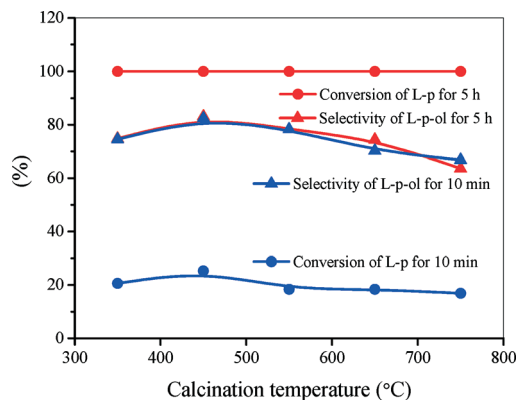


Fig. 9 Effect of the calcination temperature (t) on the performance of the CZA-d-2- t catalyst for the hydrogenation of L-phenylalanine methyl ester at 110 °C and 4 MPa of H₂ for 10 min and 5 h (L-p/Cat. = 1.5, wt.).

hardly changed (~83.6%) and the conversion of L-phenylalanine methyl ester is gradually increased with the reaction time. The conversion reaches 98.3% for 2 h and 100% for 3 h.

The physicochemical data in Table 4 show that the BET surface area of CZA-d-2- t is decreased from 125 to 39.9 m² g⁻¹ with an increase in calcination temperature from 350 to 750 °C, while the variation trend of S_{Cu} and D_{Cu} is similar to the xBET surface area with the calcination temperature. On the

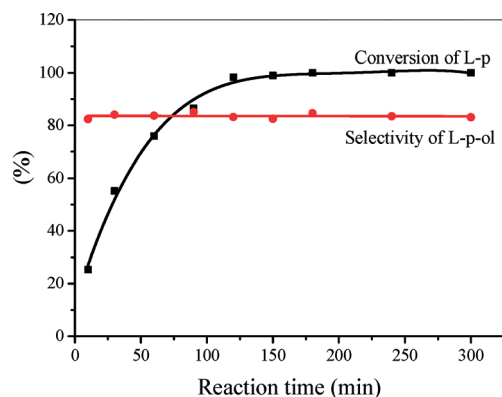


Fig. 10 The effect of reaction time on the L-phenylalanine methyl ester hydrogenation over the CZA-d-2-450 catalyst at 110 °C and 4 MPa of H₂ (L-p/Cat. = 1.5, wt.).

contrary, the average size of CuO crystallites (d_{CuO}) is increased from 9.7 nm (CZA-d-2-350) to 27.3 nm (CZA-d-2-750). The growth of crystal grain (and/or the agglomeration of particles) and the formation of spinel oxide are closely related to the calcination temperature, resulting in the variation of S_{BET} , S_{Cu} , D_{Cu} and d_{CuO} .⁴⁴

Comparing with CZA-d-2-350, CZA-d-2-450 with lower surface area and S_{Cu} exhibits the higher catalytic performance, indicating that S_{Cu} is not the sole decisive factor for the catalytic performance of Cu/ZnO/Al₂O₃. Spencer *et al.*⁴⁷ proposed that hydrogen dissociation on zinc oxide, followed by hydrogen spillover to copper, is significant for the Cu/ZnO/Al₂O₃ catalysts. Sun *et al.*^{49,50} found that the strength and nature of the interaction between dispersed copper and other oxide species rather than only their surface area are decisive for the catalytic activity, such as the reported Cu/ZrO₂ catalyst. Wu *et al.*⁵¹ suggested that the encapsulation effect becomes apparent with an increase in the calcination temperature, which can reinforce the interaction between metallic copper and zirconia in the Cu/ZrO₂ catalysts. And undesired aggregations would occur under relatively high calcination temperatures. Thus, we speculate that the interaction between CuO and ZnO plays an important role in the catalytic activity, and the role of ZnO in the Cu/ZnO/Al₂O₃ catalyst cannot be ignored. It is reasonable that the CZA-d-2-350 sample with the largest S_{Cu} is not related to the highest catalytic performance, because of the weaker interaction between metallic copper and ZnO when the calcination temperature is too low. In addition, the Tammann temperature of CuO is only 558 °C;⁵² too high calcination temperature might result in the sintering of CuO crystallites. Therefore, the calcination temperature of 450 °C is appropriate for the Cu/ZnO/Al₂O₃ catalyst.

The XRD patterns of the catalysts calcined at different temperatures are shown in Fig. 11. It can be seen that no diffraction peaks of the Al₂O₃ and ZnO phases can be observed for all samples, which is similar to the results in Fig. 2 and 6 (the effects of precipitation methods and aging time). Weaker and broader diffraction peaks of CuO (JCPDS 80-1268) appear at $2\theta = 35.5^\circ$ and 38.8° in the XRD curve of CZA-d-2-350. With an increase in the calcination temperature, the diffraction peaks of the CuO phase become stronger and sharper, indicating an increase in the crystallization degree of CuO. After this catalyst was calcined at 550 °C, the

Table 4 Physicochemical properties of the Cu/ZnO/Al₂O₃ catalysts calcined at different temperatures

Catalyst	Calcination temp. (°C)	Molar composition ^a			S_{BET} (m ² g ⁻¹)	d_{CuO} (nm)	S_{Cu} (m ² g ⁻¹)	D_{Cu} ^b (%)	TOF × 10 ^{3c} (s ⁻¹)	S_{Cu} :TOF (m ² s ⁻¹ g ⁻¹)	B-TOF ^d (s ⁻¹)
		Cu	Zn	Al							
CZA-d-2-350	350	1.02	0.31	1.01	125	9.7	24.5	11.7	3.5	0.0637	0.052
CZA-d-2-450	450	1.03	0.29	0.98	92.0	10.2	16.9	8.1	7.0	0.120	0.114
CZA-d-2-550	550	1.01	0.31	1.00	82.1	18.3	12.9	6.2	7.9	0.102	0.246
CZA-d-2-650	650	1.03	0.32	1.06	47.6	23.9	6.8	3.3	10.7	0.073	0.415
CZA-d-2-750	750	1.00	0.30	1.01	39.9	27.3	4.8	2.3	13.3	0.064	0.576

^a Determined by the ICP-OES method. ^b D_{Cu} = exposed Cu atoms/total Cu atoms. ^c Turnover frequency (TOF) represents the number of L-phenylalaninol molecules formed (reaction for 10 min) per second per surface metallic copper atom. ^d B-TOF represents the number of L-phenylalaninol molecules formed (reaction for 10 min) per second per Cu⁰ atom in the boundary between CuO and ZnO or Al₂O₃.

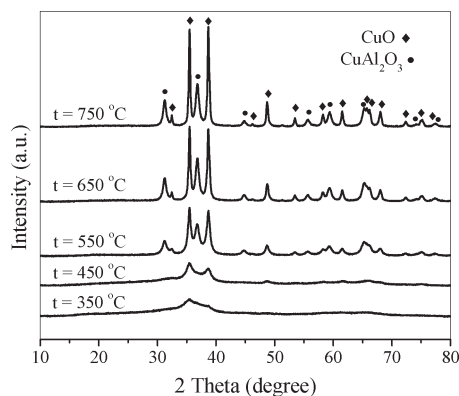


Fig. 11 XRD patterns of the CZA-d-2-*t* catalysts calcined at different temperatures (*t*).

CuAl₂O₄ spinel phase was formed, and its diffraction peaks (JCPDS 33-0448) are located at $2\theta = 31.2^\circ$, 36.8° , 44.8° and 55.7° (Fig. 11). The higher the calcination temperature is, the higher the crystallization degree of CuAl₂O₄ produced. After calcination at 750 °C, the CZA-d-2-750 sample was agglomerated significantly (Fig. 12).

The H₂-TPR profiles of the CZA-d-2-*t* calcined at different temperatures are shown in Fig. 13. It can be seen that all of the Cu/ZnO/Al₂O₃ catalysts exhibit a broad peak of H₂ consumption at 150–275 °C, which can be deconvoluted into two peaks (α and β peaks). The positions and the contributions of these reduction peaks are summarized in Table 5. Since ZnO, Al₂O₃ and CuAl₂O₃ cannot be reduced at <350 °C, the peaks of H₂ consumption are ascribed to the reduction of

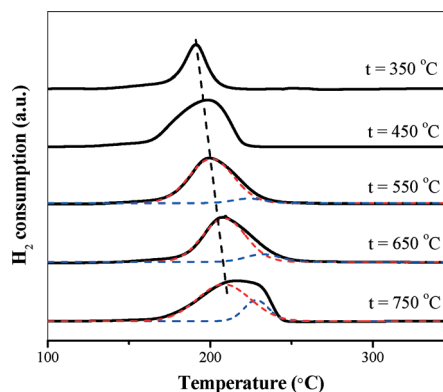


Fig. 13 H₂-TPR profiles of the CZA-d-2-*t* catalysts calcined at different temperatures (*t*).

Table 5 The top temperatures of reduction peaks and their contributions to TPR patterns of Cu/ZnO/Al₂O₃ calcined at different temperatures

Catalyst	T_α (°C)	T_β (°C)	$A_\alpha/(A_\alpha + A_\beta)^a$ (%)
CZA-d-2-750	209	228	79.0
CZA-d-2-650	207	232	87.9
CZA-d-2-550	201	224	93.3
CZA-d-2-450	196	—	~100
CZA-d-2-350	191	—	100

^a A_α and A_β represent the area of α and β peaks, respectively.

CuO species.⁴⁵ The results show that decreasing the calcination temperature causes the positions of the reduction peaks to shift toward lower temperatures accompanied by an increase in the fraction of the α peak, which indicates that the amount of easily reducible well-dispersed copper oxide increases with a decline in the calcination temperature. For the sample calcined at 350 °C, its reduction peak reaches the lowest temperature and its peak area is also the smallest, which should be ascribed to a large amount of nano-CuO species encapsulated in bulk of the catalyst due to a higher dispersion degree and smaller crystallites of CuO (Table 4).

4. Turnover frequency (TOF) of L-phenylalaninol formation

To better understand the nature of the activity of the catalyst active sites, the turnover frequency (TOF) of L-phenylalaninol formation was used, which means the number of L-phenylalaninol molecules formed per second per surface metallic copper atom on the basis of the surface area of metallic Cu⁰ (S_{Cu}). The results in Fig. 10 show that the reactant conversion is close to 100% after 2 h of reaction. To appropriately compare the activity of the active sites of different catalysts in the kinetic region, the TOFs were calculated on the basis of formed L-phenylalaninol after 10 min of reaction (that is the data during the initial 10 min), and the results are listed in Tables 1, 3 and 4.

Fig. 14A shows the relationship between TOF and the mean particle size of CuO (d_{CuO}) calculated using the

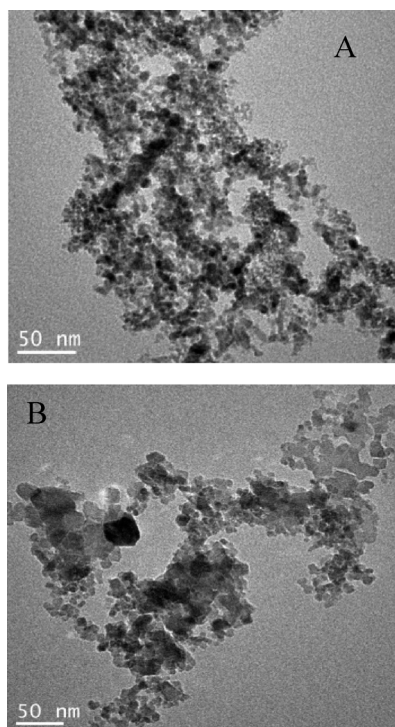


Fig. 12 TEM images of (A) CZA-d-2-450 and (B) CZA-d-2-750.

Scherrer equation on the basis of the XRD spectra. The results show that the TOF value decreases with a decrease in d_{CuO} , that is to say, the larger CuO particles possess higher catalytic activities for the title reaction, because the smaller CuO particles are affected easily by ZnO (or Al_2O_3) near or exhibit stronger interaction between CuO and ZnO (or Al_2O_3). This situation has been found in the CuO–ZnO/ ZrO_2 catalyst for CO_2 hydrogenation to produce methanol^{41,53} and indicates also the structure-sensitive catalytic hydrogenation character of the title reaction.

TOF against the metallic copper surface area (S_{Cu}) was also plotted in Fig. 14B. The results show that TOF of L-phenylalaninol formation decreases with an increase in S_{Cu} , which indicates a decrease in utilization of individual copper atoms. This result suggests that the activity of the catalyst is not only related to S_{Cu} but also to other causes.

In our previous works, the L-phenylalaninol selectivity over the CuO/ Al_2O_3 catalyst was only 10.7%, and after adding ZnO in the CuO/ Al_2O_3 catalyst, the L-phenylalaninol selectivity was increased obviously.³⁰ This suggests that ZnO is a very important promoter of the CuO/ Al_2O_3 catalyst for this reaction. Therefore, TOF over the Cu/ZnO/ Al_2O_3 catalyst is not only dependent on S_{Cu} and d_{CuO} but also on the synergetic effect or interaction between the metallic copper and the other oxide components, such as ZnO and Al_2O_3 .

Herein, the CZA-d-2-450 catalyst is the most efficient for the title reaction, but its TOF is only $7.0 \times 10^{-3} \text{ s}^{-1}$, why? This

is because the activity of the Cu-based catalyst is not only related to the catalytic activity of individual copper atoms (TOF) but also to the total number of copper atoms on the catalyst surface, namely, the surface area of Cu^0 (S_{Cu}) on the catalyst. The larger the S_{Cu} , the greater the number of active sites on the catalyst surface. If the S_{Cu} ·TOF values of catalysts were compared, we find that S_{Cu} ·TOF of the CZA-d-2-450 catalyst is the largest ($0.120 \text{ m}^2 \text{ s}^{-1} \text{ g}^{-1}$) among all of the Cu/ZnO/ Al_2O_3 catalysts (Table 4).

It is well known that the catalytic activities of Cu/ZnO/ Al_2O_3 catalysts are not only dependent on the number of active sites but also on the Cu dispersion and interaction of Cu/Zn. However, the active sites of the catalysts are still controversial, and many different (and conflicting) models have been proposed by different researchers.^{54,55} Many researchers (including us) thought that the atoms or sites in the boundary (or interface) between the A component and the B component (or the active component and support) are mainly catalytic active sites for the supported catalysts,^{56,57} such as the Cu/ZnO/ Al_2O_3 catalyst.

In general, TOF is calculated on the basis of all surface metallic atoms or sites, but many surface atoms or sites are inactive. Hence, the obtained value of TOF often is much lower. Herein, we propose the turnover frequency on the basis of the active sites in the boundary, defined as B-TOF, because the interaction between different oxides (or metal and support) occurs in the boundary or interface. Once this

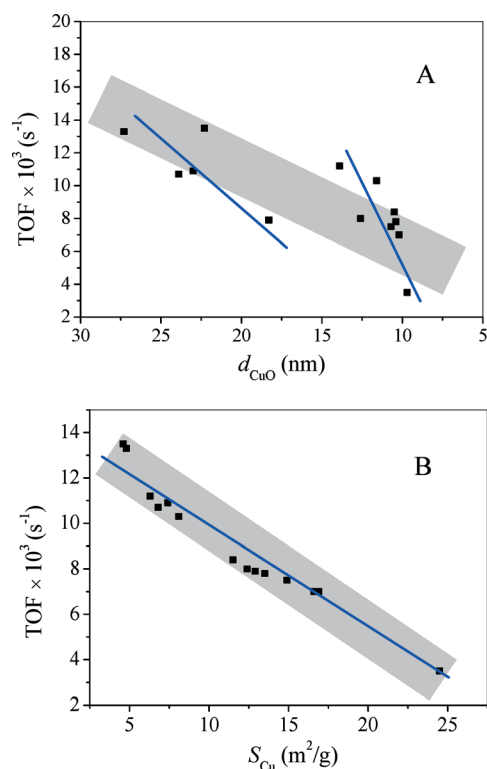


Fig. 14 The relationship between TOF of L-phenylalaninol formed and (A) the mean particle size of CuO (d_{CuO}) and (B) the surface area of Cu^0 (S_{Cu}) on the Cu/ZnO/ Al_2O_3 catalysts (reaction condition: 110 °C and 4 MPa of H_2 for 10 min, L-p/Cat. = 1.5, wt.).

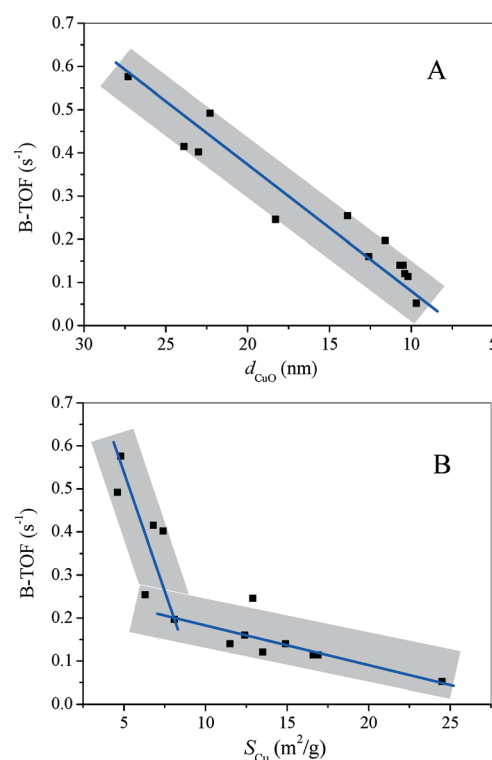


Fig. 15 The relationship between B-TOF of L-phenylalaninol formed and (A) the mean particle size of CuO (d_{CuO}) and (B) the surface area of Cu^0 (S_{Cu}) on the Cu/ZnO/ Al_2O_3 catalysts (reaction condition: 110 °C and 4 MPa of H_2 for 10 min, L-p/Cat. = 1.5, wt.).

hypothesis can be demonstrated by experimental evidence, the B-TOF would be widely applied because it can reflect more realistically the relationship between the catalytic activity and active sites. Herein, B-TOF means the number of L-phenylalaninol molecules formed per second per metallic copper atom in the boundary between CuO and ZnO or Al₂O₃. The results are listed in Tables 1, 3 and 4. Fig. 15 shows the relationships between B-TOF and d_{CuO} (and S_{Cu}), like the relationships of TOF against d_{CuO} (and S_{Cu}) in Fig. 14.

The results above show that B-TOF values are remarkably larger than TOF values, as the amount of B-sites are less than that of the surface active sites. For the particle size of CuO (d_{CuO}), B-TOF decreases with a decrease in d_{CuO} , that is to say, the larger CuO particles possess higher catalytic activities for the title reaction. For the surface area of Cu⁰ (S_{Cu}), B-TOF decreases with an increase in S_{Cu} , which is similar to the situation of TOF against d_{CuO} and S_{Cu} . Unlike TOF, the effects of d_{CuO} and S_{Cu} on B-TOF are more obvious, which should be attributed to the sample with bigger particles having shorter border line, resulting in less B-sites and a higher B-TOF value.

5. Conclusions

In summary, the CuZn_{0.3}AlO_x (CZA) catalysts were prepared by different precipitation methods, and their physicochemical properties are greatly affected by the preparation method and conditions. The uniform size distribution of CuO species can be obtained by fractional co-precipitation. The appropriate aging time is 2 h, and the catalyst aged for 2 h has the largest metallic copper surface area (S_{Cu}) and surface copper amount and the smallest CuO crystallites. The lower calcination temperature is favorable for increasing the surface area and metallic copper surface area of the catalyst, and the CuAl₂O₄ spinel phase would form after calcination at 550 °C. The catalytic hydrogenation activity of the Cu/ZnO/Al₂O₃ catalysts not only greatly depends on the metallic copper surface area but also on the interaction between the metallic copper and zinc oxides.

The Cu/ZnO/Al₂O₃ catalyst (CZA-d-2-450) prepared by fractional co-precipitation with aging at 70 °C for 2 h and calcination at 450 °C for 4 h shows the highest activity for L-phenylalanine methyl ester hydrogenation to L-phenylalaninol. As the catalytic activity is related to the surface area of Cu⁰ (S_{Cu}) of the catalyst and TOF, the S_{Cu} -TOF values of the CZA-d-2-450 catalyst is the largest (0.120 m² s⁻¹ g⁻¹) among all of the Cu/ZnO/Al₂O₃ catalysts. Over this catalyst, L-phenylalanine methyl ester was hydrogenated at 110 °C and 4 MPa of H₂ for 2 h, and 83.6% selectivity to L-phenylalaninol without racemization was achieved. Further investigations regarding the catalytic reaction mechanism and deactivation and regeneration of the catalysts are in progress and will be reported in due course. Since the Cu/ZnO/Al₂O₃ catalyst is very cheap and easily prepared, this catalyst can be used widely in this selective hydrogenation.

Acknowledgements

We would like to acknowledge the financial support from the National Basic Research Program of China (2010CB732300), the ‘‘ShuGuang’’ Project (10GG23) and the Leading Academic Discipline Project (J51503) of Shanghai Municipal Education Commission and Shanghai Education Development Foundation, and The School to Introduce Talents Project (YJ2011-46).

Notes and references

- 1 V. Farina, J. T. Reeves, C. H. Senanayake and J. J. Song, *Chem. Rev.*, 2006, **106**, 2734.
- 2 J. Joossens, P. Van der Veken, A. M. Lambeir, K. Augustyns and A. Haemers, *J. Med. Chem.*, 2004, **47**, 2411.
- 3 W. Kuriyama, Y. Ino, O. Ogata, N. Sayo and T. Saito, *Adv. Synth. Catal.*, 2009, **352**, 92.
- 4 E. Corey, R. K. Bakshi and S. Shibata, *J. Am. Chem. Soc.*, 1987, **109**, 5551.
- 5 G. J. Lee, T. H. Kim, J. N. Kim and U. Lee, *Tetrahedron: Asymmetry*, 2002, **13**, 9.
- 6 A. Lattanzi, *Org. Lett.*, 2005, **7**, 2579.
- 7 C. Palomo, M. Oiarbide and A. Laso, *Angew. Chem., Int. Ed.*, 2005, **44**, 3881.
- 8 Z. Shan and W. Ha, *Lett. Org. Chem.*, 2008, **5**, 79.
- 9 G. Zhong, J. Fan and C. F. Barbas III, *Tetrahedron Lett.*, 2004, **45**, 5681.
- 10 I. Cepanec, M. Litvić, H. Mikuldaš, A. Bartolinčić and V. Vinković, *Tetrahedron*, 2003, **59**, 2435.
- 11 K. D. Parghi, S. R. Kale, S. S. Kahandal, M. B. Gawande and R. V. Jayaram, *Catal. Sci. Technol.*, 2013, **3**, 1308.
- 12 N. Azizi and M. R. Saidi, *Tetrahedron*, 2007, **63**, 888.
- 13 M. W. Robinson, A. M. Davies, I. Mabbett, T. E. Davies, D. C. Apperley, S. H. Taylor and A. E. Graham, *J. Mol. Catal. A: Chem.*, 2010, **329**, 57.
- 14 Z. Wang, Y. T. Cui, Z. B. Xu and J. Qu, *J. Org. Chem.*, 2008, **73**, 2270.
- 15 A. Abiko and S. Masamune, *Tetrahedron Lett.*, 1992, **33**, 5517.
- 16 R. Goncalves, A. Pinheiro, E. da Silva, J. da Costa, C. Kaiser and M. de Souza, *Synth. Commun.*, 2011, **41**, 1276.
- 17 M. Souček, J. Urban and D. Šaman, *Collect. Czech. Chem. Commun.*, 1990, **55**, 761.
- 18 W. Chen, J. Lu, Z. X. Shen, J. Lang, L. Zhang and Y. Zhang, *Chin. J. Chem.*, 2003, **21**, 192.
- 19 M. Studer, S. Burkhardt and H. U. Blaser, *Adv. Synth. Catal.*, 2002, **343**, 802.
- 20 S. Antons, A. S. Tilling and E. Wolters, *US Patents*, 6355848, 2002.
- 21 S. Antons, A. S. Tilling and E. Wolters, *US Patents*, 6310254, 2001.
- 22 Y. Ino, W. Kuriyama, O. Ogata and T. Matsumoto, *Top. Catal.*, 2010, **53**, 1019.
- 23 H. Adkins, *Org. React.*, 2011.
- 24 T. Turek, D. Trimm and N. Cant, *Catal. Rev.: Sci. Eng.*, 1994, **36**, 645.
- 25 P. Guo, L. Chen, S. Yan, W. Dai, M. Qiao, H. Xu and K. Fan, *J. Mol. Catal. A: Chem.*, 2006, **256**, 164.

- 26 L. F. Chen, P. J. Guo, L. J. Zhu, M. H. Qiao, W. Shen, H. L. Xu and K. N. Fan, *Appl. Catal., A*, 2009, **356**, 129.
- 27 Y. Yu, Y. Guo, W. Zhan, Y. Guo, Y. Wang, Y. Wang, Z. Zhang and G. Lu, *J. Mol. Catal. A: Chem.*, 2011, **337**, 77.
- 28 P. Yuan, Z. Liu, W. Zhang, H. Sun and S. Liu, *Chin. J. Catal.*, 2010, **31**, 769.
- 29 D. S. Brands, E. K. Poels and A. Blik, *Appl. Catal., A*, 1999, **184**, 279.
- 30 C. Y. Gao, X. Z. Xiao, D. S. Mao and G. Z. Lu, *Catal. Sci. Technol.*, 2013, **3**, 1056.
- 31 T. Yurieva, *React. Kinet. Catal. Lett.*, 1995, **55**, 513.
- 32 J. L. Li and T. Inui, *Appl. Catal., A*, 1996, **137**, 105.
- 33 R. T. Figueiredo, H. M. C. Andrade and J. L. Fierro, *J. Mol. Catal. A: Chem.*, 2010, **318**, 15.
- 34 H. Jung, D. R. Yang, O. S. Joo and K. D. Jung, *Bull. Korean Chem. Soc.*, 2010, **31**, 1241.
- 35 S. I. Fujita, S. Moribe, Y. Kanamori, M. Kakudate and N. Takezawa, *Appl. Catal., A*, 2001, **207**, 121.
- 36 H. Usuki, Y. Yamamoto, J. Arima, M. Iwabuchi, S. Miyoshi, T. Nitoda and T. Hatanaka, *Org. Biomol. Chem.*, 2011, **9**, 2327.
- 37 L. C. Wang, Q. Liu, M. Chen, Y. M. Liu, Y. Cao, H. Y. He and K. N. Fan, *J. Phys. Chem. C*, 2007, **111**, 16549.
- 38 G. Avgouropoulos, T. Ioannides and H. Matralis, *Appl. Catal., B*, 2005, **56**, 87.
- 39 W. H. Cheng, *Appl. Catal., A*, 1995, **130**, 13.
- 40 I. Melián-Cabrera, M. López Granados and J. Fierro, *J. Catal.*, 2002, **210**, 273.
- 41 X. M. Guo, D. S. Mao, G. Z. Lu, S. Wang and G. S. Wu, *J. Catal.*, 2010, **271**, 178.
- 42 F. Arena, K. Barbera, G. Italiano, G. Bonura, L. Spadaro and F. Frusteri, *J. Catal.*, 2007, **249**, 185.
- 43 I. Melian-Cabrera, M. L. Granados and J. Fierro, *J. Catal.*, 2002, **210**, 285.
- 44 X. Guo, D. Mao, S. Wang, G. Wu and G. Lu, *Catal. Commun.*, 2009, **10**, 1661.
- 45 H. Yahiro, K. Nakaya, T. Yamamoto, K. Saiki and H. Yamaura, *Catal. Commun.*, 2006, **7**, 228.
- 46 Q. Sun, Y. L. Zhang, H. Y. Chen, J. F. Deng, D. Wu and S. Y. Chen, *J. Catal.*, 1997, **167**, 92.
- 47 M. Spencer, *Top. Catal.*, 1999, **8**, 259.
- 48 B. L. Kniep, F. Girgsdies and T. Ressler, *J. Catal.*, 2005, **236**, 34.
- 49 Y. Sun and P. A. Sermon, *J. Chem. Soc., Chem. Commun.*, 1993, 1242.
- 50 Y. Sun and P. A. Sermon, *Catal. Lett.*, 1994, **29**, 361.
- 51 G. Wu, Y. Sun, Y. W. Li, H. Jiao, H. W. Xiang and Y. Xu, *J. Mol. Struct.: THEOCHEM*, 2003, **626**, 287.
- 52 R. Baker and J. Chludzinski, *Carbon*, 1981, **19**, 75.
- 53 F. Arena, G. Italiano, K. Barbera, G. Bonura, L. Spadaro and F. Frusteri, *Catal. Today*, 2009, **143**, 80.
- 54 K. Klier, *Adv. Catal.*, 1982, **31**, 243.
- 55 P. L. Hansen, J. B. Wagner, S. Helveg, J. R. Rostrup-Nielsen, B. S. Clausen and H. Topsøe, *Science*, 2002, **295**, 2053.
- 56 M. Behrens, F. Studt, I. Kasatkin, S. Köhl, M. Hävecker, F. Abild-Pedersen, S. Zander, F. Girgsdies, P. Kurr and B. L. Kniep, *Science*, 2012, **336**, 893.
- 57 Y. Y. Wu, N. A. Mashayekhi and H. H. Kung, *Catal. Sci. Technol.*, 2013, **3**, 2881.